Orienting Block Copolymer Microdomains with Block Copolymer Brushes

Weiyin Gu, Sung Woo Hong,[†] and Thomas P. Russell[*]

Department of Polymer Science & Engineering, University of Massachusetts, 120 Governors Drive, Amherst, Massachusetts 01003-4530, United States. [†]Present address: Samsung Advanced Institute of Technology (SAIT), Mt. 14-1, Nongseo-dong, Giheung-gu, Yongin-si, Gyeonggi-do 446-712, Republic of Korea.

ABSTRACT A simple, rapid, and robust technique for controlling the self-assembly of block copolymers (BCPs) with a large segmental interaction parameter, χ, is described using a surface modified with anchored BCP brushes. End-functionalized poly(styrene-*b*-ethylene oxide)s (PS-*b*-PEOs), where the fraction of PS (f_{PS}) was varied, end-functionalized neat PS, and end-functionalized neat PEO were end-grafted onto Si substrates modifying the surface with polymer brushes. Thin films of cylinder-forming PS-*b*-PEO were prepared on modified Si substrates and thermally annealed. When neat PS and PEO were used as the anchored brushes, the microdomains of the PS-*b*-PEO oriented parallel to the substrate upon thermal annealing due to the preferential interactions of one block to the anchored brushes. However, when end-functionalized PS-*b*-PEOs were used to modify the substrate, hexagonally packed cylindrical PEO microdomains oriented normal to the substrate, having long-range lateral ordering, were obtained over a very wide range of f_{PS} (0.32 to 0.77).

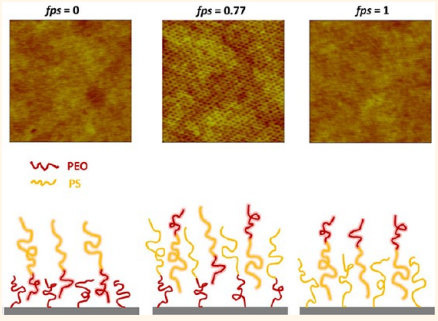

KEYWORDS: block copolymer thin film · polymer brushes · substrate modification · controlled orientation

Block copolymers (BCPs) have extensively been investigated because of their ability to self-assemble into well-ordered arrays of nanoscopic structures with periodicities on the tens of nanometer size scale. In particular, thin films of BCPs hold promise for new technological breakthroughs, since they can be used as templates and scaffolds for ultrafiltration membranes,[1] photonic band gap materials,[2,6] nanolithographic templates and scaffolds,[3] high-density storage media,[4] and energy conversion.[5] For some applications requiring addressability, the BCP microdomains must be perfectly aligned laterally and oriented normal to the film surface. To that end, external forces like solvent annealing,[6,7] thermal annealing,[8] electromagnetic fields,[9] shear,[10] zone-annealing,[11] and topographically and/or chemically patterned substrates,[3,7,12−22] are required to guide the self-assembly process. Among them, solvent annealing and thermal annealing have widely been used, since they are simple and straightforward and can be used in combination with other external forces to enhance the lateral ordering and orientation of the BCP microdomains. However, since the choice of proper solvent is often difficult and a solvent environment can be prohibitive in a fabrication process, thermal annealing is more attractive. Due to the preferential interactions between the substrate and one of the blocks and the difference in the surface energies of the blocks, thermal annealing generally promotes orientation of the microdomains parallel to the surface. To control the orientation of thermally annealed BCP microdomains, self-assembled monolayers (SAMs) or modification of the substrate with random copolymers has been used to tune the interfacial interactions at the substrate.[21−23] For example, the surface energy of the substrate can be tuned by adjusting the composition of a random copolymer that is either grafted to substrates to form a brush layer or coated onto the substrate and cross-linked to form a mat.[24,25] Mansky *et al.* showed that the substrate modified by a hydroxyl-terminated poly(styrene-*r*-methyl methacrylate) (P(S-*r*-MMA)) copolymer with a styrene fraction of 0.57 ± 0.05 is nonpreferential to PS and PMMA blocks and, thus, promotes the orientation of the microdomains of polystyrene-*b*-poly(methyl methacrylate) (PS-*b*-PMMA) normal

* Address correspondence to tprussell@mail.pse.umass.edu.

Received for review September 2, 2012 and accepted October 23, 2012.

Published online October 23, 2012
10.1021/nn304049w

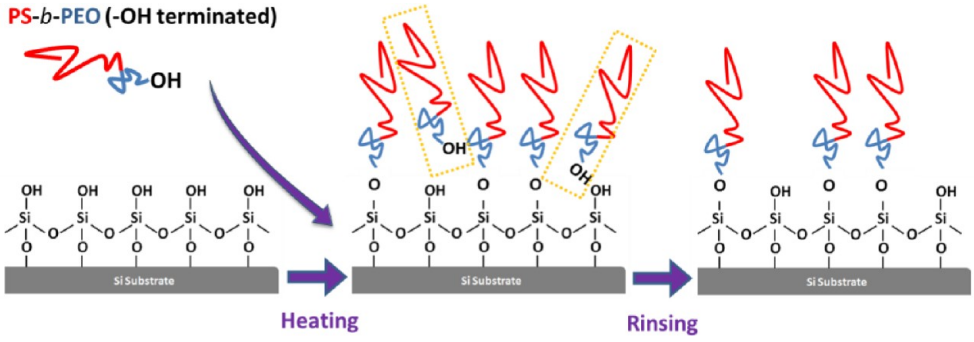

Scheme 1. Diagrammatic representation for the surface modification of Si substrates with block copolymers.

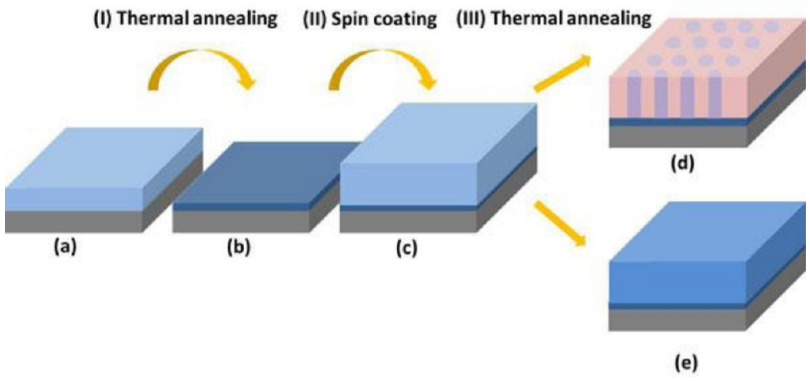

Scheme 2. (a) Thin films composed of hydroxyl-terminated homopolymers or hydroxyl-terminated BCPs are prepared on Si substrates; (b) an anchored brush layer was left on the Si substrates after thermal annealing followed by successive solvent washing; (c) thin films of PS-*b*-PEO (S32EO11) are prepared on the anchored brush layer; (d) highly ordered hexagonal arrays oriented normal to the substrate are achieved after thermal annealing on the BCP brushes; (e) microdomains oriented parallel to the substrate are achieved after thermal annealing on the homopolymer brushes.

to the film surface.[22] There are three important advantages to this strategy: (1) since the surface energy difference between PS and PMMA is not significant, a relatively wide processing window of P(S-*r*-MMA) is possible to orient the microdomains of PS-*b*-PMMA normal to the substrate; (2) the synthesis of P(S-*r*-MMA) is straightforward; and (3) a polymer or BCP film placed on the surface of the brushes adheres well to the substrate since it penetrates into the anchored brush. However, with many other BCPs, such as polystyrene-*b*-poly(ethylene oxide) (PS-*b*-PEO), polyisoprene-*b*-polylactide (PI-*b*-PLA), and polystyrene-*b*-poly(vinylpyridine) (PS-*b*-PVP), this strategy is not suitable due to the difficulty in synthesis of the corresponding end-functionalized random copolymer or the large differences in the surface energies of the blocks, which forces an orientation of the microdomains parallel to the surface. For these reasons, there are few examples where this strategy has been used with BCPs where χ between the blocks was large. Recently, Ji *et al*. reported that orientation of the microdomains in PS-*b*-P2VP thin films normal to the film surface could be achieved with poly(styrene-*r*-2-vinylpyridine-*r*-hydroxyethyl methacrylate) (P(S-*r*-2VP-*r*-HEMA)) random copolymer brushes. However, the orientation of the P2VP microdomains normal to the surface was achieved only over a very narrow range of styrene fractions (0.48 to 0.57) in the P(S-*r*-2VP-*r*-HEMA) brushes. In addition, the thin films must be confined between two substrates having P(S-*r*-2VP-*r*-HEMA) brushes attached to each interface.[26]

Here, we investigate the use of BCP brushes, rather than random copolymer brushes, to control the orientation of BCP microdomains in thin films. PS-*b*-PEO is chosen as a representative model, where χ is large between the S and EO segments. For preparing both the brush layers and BCP thin films, we use commercially available PS-*b*-PEOs having hydroxyl groups at the end of the PEO block, which enables the BCPs to be covalently anchored to the native oxide layer on a silicon substrate (Scheme 1).[27] We also investigate the dependence of the orientation of the BCP microdomains on the composition of the anchored BCP brushes.

RESULTS AND DISCUSSION

The method used to produce ordered microdomains of block copolymers on the surface of polymer brushes is shown in Scheme 2.

A series of end-functionalized BCPs of PS-*b*-PEO with different composition ratios (see Materials in Experimental Section and Table 1), where a hydroxyl group

TABLE 1. Sample Designations of Polymers Used to Modify Si Substrates

	PEO	S12E030	S21.5E020	S32E011	PS
f_{PS}	0	0.32	0.55	0.77	1

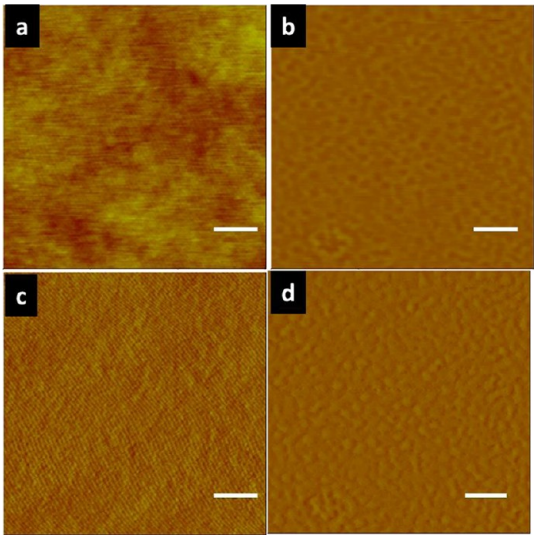

Figure 1. Height (a, b) and phase (c, d) mode SFM images of S32EO11-modified Si substrates before (a, c) and after (b, d) rinsing with toluene and chloroform. Scale bar: 250 nm.

was attached to the end of PEO block, were used to generate the BCP brushes. For simplicity, PS-*b*-PEOs were coded with the molecular weights of each block (see Materials in Experimental Section). As a reference, hydroxyl-terminated polystyrene (PS) or poly(ethylene oxide) (PEO) was also used to generate homopolymer brushes.

Films of the hydroxyl-terminated PS-*b*-PEOs were spin coated onto Si substrates. The concentrations of the solutions used for spin coating were such that the initial film thickness was ~50 nm. Upon heating, the PEO block preferentially segregates to the substrate interface (as would a nonfunctionalized BCP), and, for those PEO blocks with the end-functionalized hydroxyl group close to the substrate, the hydroxyl groups react with the native oxide layer on the Si substrate, anchoring only those chains to the substrate whose chain ends are in close proximity to the substrate, as shown in Scheme 1. After reaction, the thermally annealed film was thoroughly rinsed with chloroform and toluene to remove the unanchored polymers, leaving Si substrates with a native oxide layer that is modified with PS-*b*-PEO brushes. The same procedure was used to prepare Si substrates modified with neat PS brushes or PEO brushes.

Figure 1 shows scanning force microscopy (SFM) images of the Si substrates modified by S32EO11 brushes.

When a thin film of end-functionalized S32EO11 is coated onto the surface of a silicon substrate (Figure 1a and c) and thermally annealed, the PEO preferentially

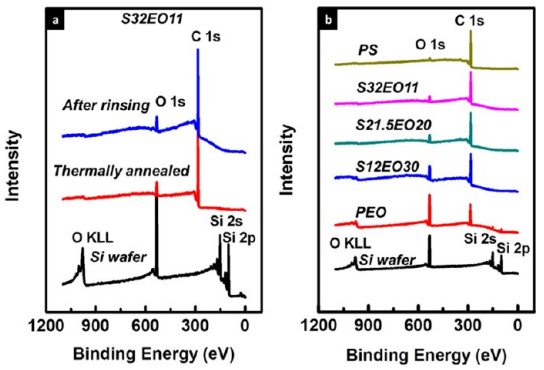

Figure 2. XPS survey spectra of modified Si substrates.

interacts with the substrate, and the PS, due to its lower surface energy, is preferentially located at the top surface. So, if the film is $L_0/2$ or $3L_0/2$ in thickness (L_0 = the lattice spacing of the hexagonally packed cylindrical microdomains), there is no surface topography (hole and island) formed (due to incommensurability between the film thickness and period of the BCP) and the film is smooth with no height variation on the surface (0.5 nm rms roughness). Now, when the film is thoroughly washed (Figure 1b and d), the height image shows a surface that is relatively flat; however, there is a mottling evident (Figure 1b) where the variation in the height is small (0.8 nm in rms roughness). A similar type of mottling is seen in the phase image (Figure 1d). It should be noted that the higher area in the height image (lighter color) corresponds to the darker areas (softer areas) in the phase image. This indicates that the end-anchored BCP brush does not form a simple, uniform bilayer with PEO at the substrate, but, rather, there is some lateral variation in the coverage of the end-anchored BCP brush on the substrate. These characteristics were typical for all of the surfaces modified with the BCP brushes (see Supporting Information, Figure S1).

All the Si substrates modified with the polymer brushes were characterized by X-ray photoelectron spectroscopy (XPS) and tensiometry, as shown in Figures 2 and 3, respectively. XPS, performed at a takeoff angle of 75°, was used to determine the composition of the anchored BCP chains. Shown in Figure 2a are the spectra of a bare silicon substrate (black), a thin film of S32EO11 after thermal annealing (red), and a substrate modified with S32EO11 BCP brushes after rinsing (blue). Thin films of S32EO11, before and after rinsing, showed a disappearance of Si 2s and 2p peaks, the presence of the C 1s peak at 289.3 eV, and the suppression of the O 1s peak.[28] The disappearance of Si 2s and 2p peaks indicates that the BCP thin film fully covers the Si substrate. Similar results were also obtained for the other BCP brushes (Figure 2b), where the C 1s peak is dominant in all of the modified Si substrates, except for the one modified by the PEO brushes. The results from static contact angle measurements of

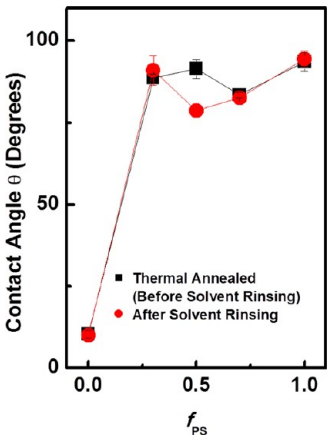

Figure 3. Contact angle measurements of modified Si substrates. f_{PS} is the volume fraction of PS in PS-*b*-PEO block copolymers.

modified Si substrates before rinsing suggested that PS segregates to the surfaces, due to its lower surface energy, as evidenced by the contact angles close to 100° (black rectangle in Figure 3), which is similar to a previous report.[29] After removing the unreacted polymers, the Si substrates modified with BCP brushes showed similar contact angles (red circle in Figure 3). XPS results (Figure 2b) are also in good agreement with the contact angle measurements.

Thin films of S32EO11 were prepared on the modified Si substrates where the thickness of the S32EO11 is $\sim L_0(2\pi/q^*)$.[30] L_0 was determined to be 29.5 nm in a previous paper.[15] Figure 4 shows SFM images of thermally annealed S32EO11 thin films on Si substrates modified by different polymer brushes.

When S32EO11 thin films were thermally annealed on Si substrates modified by PEO homopolymer brushes (Figure 4a and b), the surface of the film was featureless in both the height and phase images. This is understandable, since the constraints arising from the interfacial interactions with the PEO brush, the lower surface energy of the PS block, and the film thickness would force the BCP microdomains to orient parallel to the surface and perturb the inherent cylindrical microdomain morphology into a more lamellar-like structure. When the BCP was placed on a PS brush (Figure 4e and j), the thermally annealed BCP film is featureless in the height image (Figure 4e). However, in the phase image, the presence of the PEO microdomains beneath a thin layer of the PS can be detected and an array of cylindrical microdomains oriented parallel to the surface is observed (Figure 4j). This is expected, given the film thickness and interfacial interaction constraints placed on the BCP.

For thin films of the BCP with a thickness corresponding to L_0, which were thermally annealed on Si substrates modified with end-anchored BCPs, an unexpected result was found. Regardless of f_{PS} of the end-anchored BCP (0.32 to 0.77), the thermally annealed

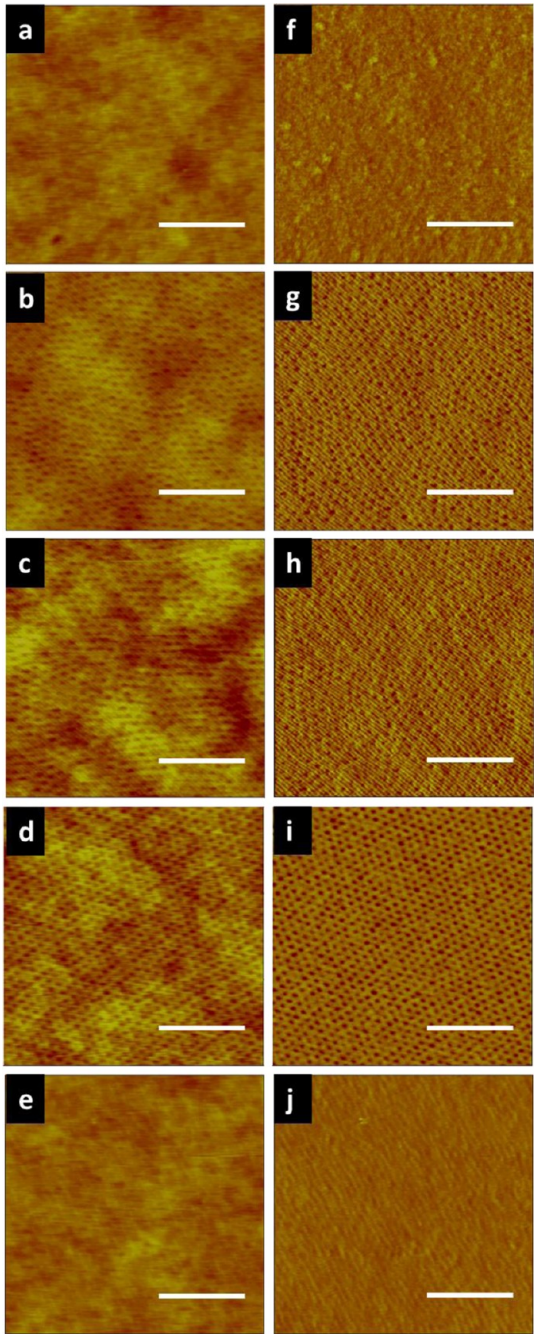

Figure 4. SFM height (a−e) and phase (f−j) images of S32EO11 thin films prepared on f_{PS} of (a) 0, (b) 0.32, (c) 0.55, (d) 0.77, and (e) 1 modified Si substrates, respectively. Scale bar: 250 nm.

BCP films formed hexagonally packed cylindrical microdomains oriented normal to the substrate. Since the contact angle results indicated the top surface was covered with PS, this result was not anticipated and can be related to the areal density of BCP chains end-anchored to the surface and the penetration of the BCP into the brush layer. The areal density of end-functionalized BCP chains anchored to the surface is less than that for the corresponding homopolymer. This results from the configurational restrictions that the microphase separation places on the end-functionalized PEO block

and the number of chain ends that are in close enough proximity to the substrate to chemically anchor to the substrate (Scheme 1). In addition to the configurational constraints, there is an inherent competition between the preferential interaction of any segment of the PEO block with the substrate and the displacement of these segments from the surface by the end-functionalized segments to enable anchoring. A careful examination of the SFM results shows that the end-functionalized homopolymers form a smooth, uniformly thick brush attached to the substrate, while the end-anchored BCPs, after removal of the nonanchored chains, show a mottling in the height and phase images where the height variations of at most several nanometers (~3 nm) are evident. While this is small, it is still a large variation in comparison to the total thickness of the brushes formed by the end-anchored BCP chains (9–11 nm). The mottling arises from an irregular, lateral microphase separation of the BCP chains anchored to the substrate, combined with preferential interactions of the PEO block with the substrate, and the preference for the PS block to the surface due to its lower surface energy. Similar constraints are not present for the end-functionalized homopolymer, and, as such, the areal densities of the end-anchored homopolymers are larger. (See Supporting Information "Grafting Density Calculation".) This variation in the areal densities of the end-functionalized chains to the substrate influences the extent to which the BCP film subsequently placed on top of the brush can penetrate into the brush. For the end-functionalized homopolymers with higher areal densities, the brushes are dense and the BCP experiences interactions with only the anchored homopolymer with little penetration. Consequently, the PEO block of the BCP preferentially wets the end-anchored PEO brush, while the PS block preferentially wets the end-anchored PS brush. This results in an orientation of the BCP microdomains parallel to the surface, as is observed. In the case of the end-functionalized BCP brushes, the reduced areal densities of the anchored chains enable the BCP to penetrate deeply into the brush and the blocks of the BCP effectively experience an averaged interaction with the anchored brush, resulting in an orientation of the BCP parallel to the substrate, on average, and an orientation of the microdomains normal to the films surface. The preferential segregation of the PS block to the air surface, due to the difference in interfacial energies, restricts the thickness of the film to being $\sim L_0$. With thicker films, a mixed orientation of the morphology may result.[31]

As shown in Figure 4b–d and 4g–i, S32EO11 self-assembled on Si substrates modified by the end-anchored PS-*b*-PEO brushes (S12EO30, S21.5EO20, and S32EO11) to form hexagonally packed cylindrical microdomains oriented normal to the substrate. From analysis of the SFM results, the center-to-center distance between adjacent cylindrical microdomains (20 nm in diameter) of PEO was 36 nm. Grazing incidence small-angle X-ray scattering (GISAXS) was also used to characterize the thin films. An incidence angle of 0.18°, which is above the critical angle of the polymer (0.16°) but below that of the silicon substrate (0.28°), was chosen so that the X-rays penetrated into the film, where the scattering profiles are characteristic of the entire film.[15] The 2D GISAXS patterns of the thermally annealed S32EO11 thin films on Si substrates modified by BCP brushes are shown in Figure 5, where q_y represents the momentum transfer normal to the incident plane, *i.e.*, parallel to the film surface, while q_z is normal to the sample surface.[15] Bragg rods (reflections extended along q_z) are seen, which is characteristic of cylindrical microdomains oriented normal to the film surface, terminated at the surface of the film.[6,7,32] Line scans in q_y are also shown in Figure 5d. All of the samples show a first-order reflection at $q^* = 0.213$ nm^{-1} and two higher order reflections at $q_2 = 0.365$ nm^{-1} ($\sqrt{3}q^*$) and $q_3 = 0.421$ ($\sqrt{4}q^*$) indicative of hexagonally packed cylindrical PEO microdomains oriented normal to the film surface. A center-to-center distance of adjacent cylinders was calculated to be 34 nm from the first-order reflection, which is consistent with the SFM results, where a domain spacing of ~36 nm would be expected.

It should be noted that, when the composition of the end-anchored BCP brush was the same as the S32EO11, the long-range lateral ordering of the microdomains was markedly enhanced in comparison to the cases where the end-anchored BCP is different from that of the film. As the fraction of PEO in the end-anchored brush decreased from 0.68 to 0.23, the diffuse background in the scattering decreased and the full width at half-maximum of the first-order reflection decreased from 0.038 nm^{-1} to 0.015 nm^{-1}, suggesting an enhancement in the lateral ordering. For Si substrates modified with S32EO11 brushes (blue curve in Figure 5d), the relative scattering vectors (q_y) of the first three peaks are found to be 1:$\sqrt{3}$:$\sqrt{4}$, indicating that a hexagonal array of cylindrical microdomains with long-range lateral ordering has developed in the films. This could be explained by a change in the configuration of the end-functionalized PEO block, which must be coupled with the preferential segregation of EO in the end-functionalized PEO block to the substrate interface. Due to the length of the PEO block in the end-functionalized BCP brushes, the areal densities of S12EO30 and S21.5EO20 brushes would be lower than that of S32EO11, indicating the effective area of unmodified substrate increased. Therefore, substrates modified with S12EO30 and S21.5EO20 brushes are more preferential to the PEO block in BCP films, which results in a less neutral environment to the BCP films in comparison to substrates modified with S32EO11.

Transmission electron microscopy (TEM) images of the BCP thin films are shown in Figure 6. The samples were stained using RuO_4 vapor at room temperature

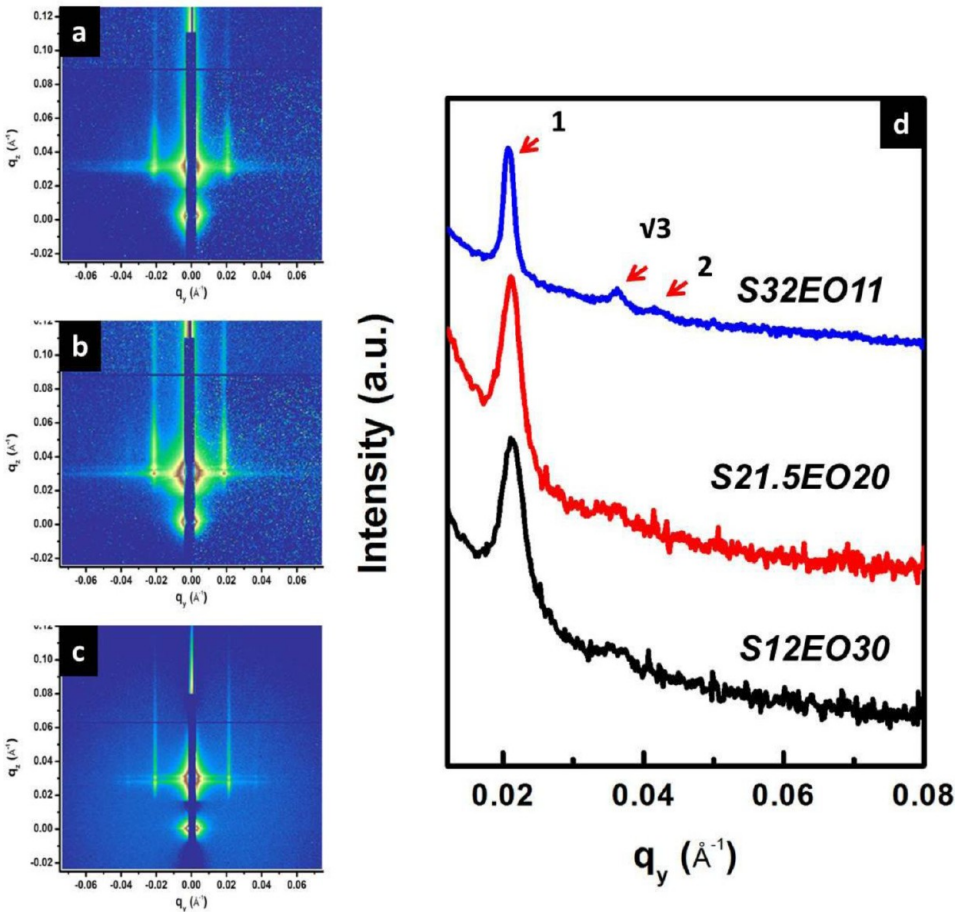

Figure 5. 2D GISAXS patterns of the thermal-annealed S32EO11 thin films (35 nm) on f_{PS} of (a) 0.32, (b) 0.55, and (c) 0.77 modified Si substrates, respectively. The linear scattering profile from a horizontal cut of (a)−(c) is shown in (d).

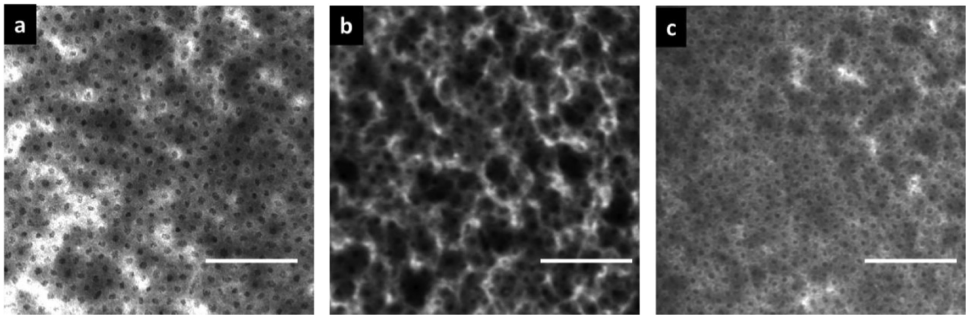

Figure 6. Transmission TEM of S32EO11 thins films prepared on f_{PS} of (a) 0.32, (b) 0.55, and (c) 0.77 modified Si substrates, respectively. Scale bar: 250 nm.

for 15 min. The PEO is selectively stained with RuO_4[32] and, therefore, appears darker than PS in the micrographs. Hexagonally packed arrays of cylindrical PEO microdomains oriented normal to the film surface are clearly evident in each of the micrographs. The average center-to-center spacing from TEM is ~38 nm, which is consistent with the SFM and GISAXS results. Cross-sectional TEM image confirmed that cylinders were oriented normal to the interface (see Supporting Information, Figure S2).

In addition to the hexagonally packed arrays of cylindrical microdomains, there is a mottled texture superposed on the image. This texture is similar to that seen in the SFM results and arises from the underlying BPC brush that was removed along with the BCP film. Since PEO is preferentially stained with RuO_4, these images clearly show the nonuniform lateral arrangement of the underlying brushes. Even though the brush BCP film uniformly coats the surface prior to and after anchoring the end-functionalized BCP to the substrate, when the nonanchored chains are removed, the remaining anchored BCP chains do not form a laterally uniform film. It is this lateral nonuniformity that enables the penetration

of the BCP into the brush and gives rise to the unexpected orientation of the BCP in contact with the brushes. It should be noted that the crystallization of the PEO limits the volume fraction of PEO that can be used and retain this morphology. If the PEO concentration is too high, the crystalline (lamellar-type) morphology will dictate the morphology of the thin film.

Control experiments were performed to highlight the necessity of using block copolymers brushes. Specifically, hydroxyl-terminated PS (M_n = 10k) and PEO (M_n = 11k) were used to modify the Si substrates sequentially. After the same S32EO11 thin film was cast and thermally annealed, although most areas were featureless, we found some spots where microdomains were oriented normal to the substrates (see Supporting Information Figure S3). This may be due to the local brush composition variation. Generally speaking, the homopolymer−mixture−brush approach is uncontrollable in terms of brush composition at a local spot, while when using block copolymers, each modified spot will have similar affinity to the above BCP layers. In addition, the former method is more time-consuming since it requires a two-step brush modification. So we believe that the block copolymer approach is unique and highly efficient. This work has not been extended to other BCP systems with larger χ parameters. However, as long as the BCP (not only PS-*b*-PEO) brushes are attached to the substrate, the same results would be obtained since the brush layers with less grafting density enable the BCP chains of film to penetrate into the brush layers, resulting in a neutral condition near the interface.

CONCLUSIONS

The development of a versatile method to control the alignment of BCP microdomains on modified Si substrates via "two-step" thermal annealing is described. This is the first report that the interactions between BCPs with a large χ and substrates could be tuned by using analogous BCP brushes that are end-anchored to the substrate, providing a new route to control the orientation and lateral ordering of BCP microdomains. Cylindrical PEO microdomains embedded in a PS matrix orientated normal to the film surface were observed in a wide processing window when the substrates were modified by PS-*b*-PEO BCPs with a volume fraction of PS, f_{PS}, varying from 0.32 to 0.77. Although the same strategy has not been extended to other BCPs with large χ parameters, this approach could be used as a useful platform methodology and would open up opportunities to fabricate highly ordered arrays of nanostructures via the self-assembly of BCP thin films.

EXPERIMENTAL SECTION

Materials. Poly(styrene-*block*-ethylene oxide)s (PS-*b*-PEOs) with different molecular weights were purchased from Polymer Source, Inc., and used as received: PS-*b*-PEO (32k-*b*-11k; the volume fraction of PS = 0.77; PDI = 1.06) (S32EO11), PS-*b*-PEO (12k-*b*-30k; the volume fraction of PS = 0.32; PDI = 1.10) (S12EO30), and PS-*b*-PEO (21.5k-*b*-20k; the volume fraction of PS = 0.55; PDI = 1.09) (S21.5EO20). In the bulk, S32EO11 self-assembled into hexagonally packed cylindrical PEO microdomains in a PS matrix with a lattice period of 33 nm, as determined by small-angle X-ray scattering. Monohydroxyl-terminated PS (10k; PDI = 1.05) and monohydroxyl-terminated PEO (41k; PDI = 1.05) were also purchased from Polymer Source, Inc. and used as received. All the polymers were dissolved in benzene, and thin films were fabricated by spin coating on a silicon substrate (International Wafer Source, Inc.). The silicon substrate was cleaned with a carbon dioxide snow jet followed by oxygen plasma treatment for 10 min.

Characterization. *Scanning Force Microscopy.* SFM images were obtained in both the height and phase-contrast mode using a Digital Instruments Dimension 3000 scanning force microscope in the tapping mode.

Grazing Incidence Small-Angle X-ray Scattering. GISAXS measurements were performed on beamline 7.3.3 at the Advanced Light Source at the Berkeley National Laboratory. An X-ray beam was impinged onto the sample at a grazing angle slightly above the critical angle of the polymer film (α_c = 0.16°) but below the critical angle of Si substrates (α_c = 0.28°). The wavelength of X-rays used was 1.240 Å, and the scattered intensity was detected by using a two-dimensional charge-coupled device (CCD) camera with image sizes of 2304 × 2304 pixels.

Transmission Electron Microscopy. For TEM in plain view, the PS-*b*-PEO film was floated off from the Si substrates onto 5 wt % HF solution and collected on a copper grid. Bright-field TEM was performed on a JEOL-2000FX TEM operating at an accelerating voltage of 200 kV.

X-ray Photoelectron Spectroscopy. XPS survey spectra were recorded using a Physical Electronics Quantum 2000 spectrometer with a 200 μm spot size, monochromatic Mg Kα excitation, and a takeoff angle of 75°. The sensitivity factors specified for the spectrometer were used for quantitative analysis. The pressure in the analysis chamber was less than 10^{-5} Pa. The spectrum collection time was kept under 10 min to minimize X-ray damage.

Tensiometry. The static water contact angle measurements of modified Si substrates were performed at room temperature (22 °C) using OCA 15 and 20 Dataphysics sessile drop tensiometers. The volume of the water droplet was kept at 15 μL, and optical images were captured 5 s after deposition.

Ellipsometry. Film thickness was measured by a Gaertner LSE ellipsometer. A He−Ne laser was used as the incident beam, with a wavelength of 632.8 nm and an incident angle of 70°.

Conflict of Interest: The authors declare no competing financial interest.

Acknowledgment. W.G., S.W.H., and T.P.R. were supported by the U.S. Department of Energy (DOE), under DOE DE-FG02-96ER45612, and W.G. also received support from the NSF-supported MRSEC at University of Massachusetts, Amherst. The authors thank L. Raboin in the NSF-supported W.M. Keck Polymer Morphology Laboratory (UMass Amherst) for assistance with the TEM measurements; Dr. Le Li and Dr. Wei Zhao for help with microtoming TEM samples preparation and measurement; and J. Hirsch in the NSF-supported Surface Analysis Facility (UMass Amherst) for assistance with XPS experiments. The authors acknowledge the use of the Advanced Light Source, Berkeley National Laboratory, which is supported by the Office of Science, Office of Basic Energy Sciences, of the U.S. Department of Energy under Contract No. DE-AC02-05CH11231.

We also acknowledge the assistance of A. Hexemer with the grazing incidence X-ray scattering measurements.

Supporting Information Available: This material is available free of charge via the Internet at http://pubs.acs.org.

Note Added after ASAP Publication: An incomplete version of Supporting Information was published with the article on October 23, 2012. The complete file published November 27, 2012.

REFERENCES AND NOTES

1. Jackson, E. A.; Hillmyer, M. A. Nanoporous Membranes Derived from Block Copolymers: From Drug Delivery to Water Filtration. *ACS Nano* **2010**, *4*, 3548–3553.
2. Fink, Y.; Urbas, A. M.; Bawendi, M. G.; Joannopoulos, J. D; Thomas, E. L. Block Copolymers as Photonic Bandgap Materials. *J. Lightwave Technol.* **1999**, *17*, 1963–1969.
3. Ruiz, R.; Kang, H.; Detcheverry, F. A.; Dobisz, E.; Kercher, D. S.; Albrecht, T. R.; de Pablo, J. J.; Nealey, P. F. Density Multiplication and Improved Lithography by Directed Block Copolymer Assembly. *Science* **2008**, *321*, 936–939.
4. Segalman, R. A. Patterning with Block Copolymer Thin Films. *Mater. Sci. Eng., R* **2005**, *48*, 191–226.
5. Orilall, M. C.; Wiesner, U. Block Copolymer Based Composition and Morphology Control in Nanostructured Hybrid Materials for Energy Conversion and Storage: Solar Cells, Batteries, and Fuel Cells. *Chem. Soc. Rev.* **2011**, *40*, 520–535.
6. Park, S.; Kim, B.; Xu, J.; Hofmann, T.; Ocko, B. M.; Russell, T. P. Lateral Ordering of Cylindrical Microdomains Under Solvent Vapor. *Macromolecules* **2009**, *42*, 1278–1284.
7. Kim, B. K.; Hong, S. W.; Park, S.; Xu, J.; Hong, S.-K.; Russell, T. P. Phase Transition Behavior in Thin Films of Block Copolymers by Use of Immiscible Solvent Vapors. *Soft Matter* **2011**, *7*, 443–447.
8. Guo, R.; Kim, E.; Gong, J.; Choi, S.; Ham, S.; Ryu, D. Y. Perpendicular Orientation of Microdomains in PS-b-PMMA Thin Films on the PS Brushed Substrates. *Soft Matter* **2011**, *7*, 6920–6925.
9. Morkved, T. L.; Lu, M.; Urbas, A. M.; Ehrichs, E. E.; Jaeger, H. M.; Mansky, P.; Russell, T. P. Local Control of Microdomain Orientation in Diblock Copolymer Thin Films with Electric Fields. *Science* **1996**, *273*, 931–933.
10. Angelescu, D. E.; Waller, J. H.; Adamson, D. H.; Deshpande, P.; Chou, S. Y.; Register, R. A.; Chaikin, P. M. Macroscopic Orientation of Block Copolymer Cylinders in Single-Layer Films by Shearing. *Adv. Mater.* **2004**, *16*, 1736–1740.
11. Berry, B. C.; Bosse, A. W.; Douglas, J. F.; Jones, R. L.; Karim, A. Orientational Order in Block Copolymer Films Zone Annealed below the Order-Disorder Transition Temperature. *Nano Lett.* **2007**, *7*, 2789–2794.
12. Bita, I.; Yang, J. K. W.; Jung, Y. S.; Ross, C. A.; Thomas, E. L.; Berggren, K. K. Graphoepitaxy of Self-Assembled Block Copolymers on Two-Dimensional Periodic Patterned Templates. *Science* **2008**, *321*, 939–943.
13. Xu, J.; Park, S.; Wang, S. L.; Russell, T. P.; Ocko, B. M.; Checco, A. Directed Self-Assembly of Block Copolymers on Two-Dimensional Chemical Patterns Fabricated by Electro-Oxidation Nanolithography. *Adv. Mater.* **2010**, *22*, 2268–2272.
14. Rockford, L.; Liu, Y.; Mansky, P.; Russell, T. P.; Yoon, M.; Mochrie, S. G. J. Polymers on Nanoperiodic, Heterogeneous Surfaces. *Phys. Rev. Lett.* **1999**, *82*, 2602–2605.
15. Park, S.; Lee, D. H.; Xu, J.; Kim, B.; Hong, S. W.; Jeong, U.; Xu, T.; Russell, T. P. Macroscopic 10-Terabit-per-Square-Inch Arrays from Block Copolymers with Lateral Order. *Science* **2009**, *323*, 1030–1033.
16. Hong, S. W.; Gu, X.; Huh, J.; Xiao, S.; Russell, T. P. Circular Nanopatterns over Large Areas from the Self-Assembly of Block Copolymers Guided by Shallow Trenches. *ACS Nano* **2011**, *5*, 2855–2860.
17. Xu, J.; Hong, S. W.; Gu, W.; Lee, K. Y.; Kuo, D S.; Xiao, S.; Russell, T. P. Fabrication of Silicon Oxide Nanodots with an Areal Density beyond 1 Teradots Inch Square. *Adv. Mater.* **2011**, *23*, 5755–5761.
18. Hong, S. W.; Huh, J.; Gu, X.; Lee, D. H.; Jo, W. H.; Park, S.; Xu, T.; Russell, T. P. Unidirectionally Aligned Line Patterns Driven by Entropic Effects on Faceted Surfaces. *Proc. Natl. Acad. Sci. U. S. A.* **2012**, *109*, 1402–1406.
19. Hong, S. W.; Russell, T. P. Chapter 7.20: Block copolymer thin films. In *Comprehensive Polymer Sciences*, 2nd ed.; Matyjaszewski, K.; Mölloer, M., Eds.; Elsevier: Oxford, in press (ISBN: 978-0-444-53349-4).
20. Hong, S. W.; Voronov, D. L.; Lee, D. H.; Hexmer, A.; Padmore, H. A.; Xu, T.; Russell, T. P. Controlled Orientation of Block Copolymers on Defect-Free Faceted Surfaces. *Adv. Mater.* **2012**, *24*, 4278–4283.
21. Kim, S. O.; Solak, H. H.; Stoykovich, M. P.; Ferrier, N. J.; de Pablo, J. J.; Nealey, P. F. Epitaxial Self-Assembly of Block Copolymers on Lithographically Defined Nanopatterned Substrates. *Nature* **2003**, *424*, 411–414.
22. Stoykovich, M. P.; Muller, M.; Kim, S. O.; Solak, H. H.; Edwards, E. W.; de Pablo, J. J.; Nealey, P. F. Directed Assembly of Block Copolymer Blends into Nonregular Device-Oriented Structures. *Science* **2005**, *308*, 1442–1446.
23. Delamarche, E.; Michel, B.; Gerber, C.; Anselmetti, D.; Guentherodt, H. J.; Wolf, H.; Ringsdorf, H. Real-Space Observation of Nanoscale Molecular Domains in Self-Assembled Monolayers. *Langmuir* **1994**, *10*, 2869–2871.
24. Mansky, P.; Liu, Y.; Huang, E.; Russell, T. P.; Hawker, C. J. Controlling Polymer-Surface Interactions with Random Copolymer Brushes. *Science* **1997**, *275*, 1458–1460.
25. Ryu, D. Y.; Shin, K.; Drockenmuller, E.; Hawker, C. J.; Russell, T. P. A Generalized Approach to the Modification of Solid Surfaces. *Science* **2005**, *308*, 236–239.
26. Ji, S.; Liu, C. C.; Son, J. G.; Gotrik, K.; Craig, G. S. W.; Gopalan, P.; Himpsel, F. J.; Char, K.; Nealey, P. F. Generalization of the Use of Random Copolymers To Control the Wetting Behavior of Block Copolymer Films. *Macromolecules* **2008**, *41*, 9098–9103.
27. Witucki, G. L. A Silane Primer: Chemistry and Applications of Alkoxy Silanes. *J. Coating Technol.* **1993**, *65*, 57–60.
28. Bacos, M. P. Carbon-Carbon Composites: Oxidation Behavior and Coatings Protection. *J. Phys. IV* **1993**, *3*, 1895–1903.
29. Kwok, D. Y.; Lam, C. N. C.; Li, A.; Zhu, K.; Wu, R.; Neumann, A. W. Low-Rate Dynamic Contact Angles on Polystyrene and the Determination of Solid Surface Tensions. *Polym. Eng. Sci.* **1998**, *38*, 1675–1684.
30. Tsui, O. K. C.; Russell, T. P. *Polymer Thin Films*; World Scientific: Singapore, 2008.
31. Kim, S. H.; Misner, M. J.; Russell, T. P. Solvent-Induced Ordering in Thin Film Diblock Copolymer/Homopolymer Mixtures. *Adv. Mater.* **2004**, *16*, 2119–2123.
32. Hui, T. R.; Chen, D. Y.; Jiang, M. A One-Step Approach to the Highly Efficient Preparation of Core-Stabilized Polymeric Micelles with a Mixed Shell Formed by Two Incompatible Polymers. *Macromolecules* **2005**, *38*, 5834–5837.
33. Huang, P.; Zheng, J. X.; Leng, S.; Van Horn, R. M.; Jeong, K.; Guo, Y.; Quirk, R. P.; Cheng, S. Z. D.; Lotz, B.; Thomas, E. L.; Hsiao, B. S. Poly(ethylene oxide) Crystal Orientation Changes in an Inverse Hexagonal Cylindrical Phase Morphology Constructed by a Poly(ethylene oxide)-block-polystyrene Diblock Copolymer. *Macromolecules* **2007**, *40*, 526–534.
34. Matyjaszewski, K.; Dong, H.; Jakubowski, W.; Pietrasik, J.; Kusumo, A. Grafting from Surfaces for "Everyone": ARGET ATRP in the Presence of Air. *Langmuir* **2007**, *23*, 4528–4531.